

Title	Promoting biological similarity by collagen microfibers in 3D colorectal cancer-stromal tissue: Replicating mechanical properties and cancer stem cell markers
Author(s)	Sasaki, Naoko; Asano, Yoshiya; Sorayama, Yukiko et al.
Citation	Acta Biomaterialia. 2024, 185, p. 161-172
Version Type	VoR
URL	<a href="https://hdl.handle.net/11094/98163">https://hdl.handle.net/11094/98163</a>
rights	This article is licensed under a Creative Commons Attribution-NonCommercial-NoDerivatives 4.0 International License.
Note	

***Osaka University Knowledge Archive : OUKA***

<https://ir.library.osaka-u.ac.jp/>

Osaka University



## Full length article

# Promoting biological similarity by collagen microfibers in 3D colorectal cancer-stromal tissue: Replicating mechanical properties and cancer stem cell markers



Naoko Sasaki<sup>a</sup>, Yoshiya Asano<sup>b</sup>, Yukiko Sorayama<sup>c</sup>, Chihiro Kamimura<sup>c</sup>, Shiro Kitano<sup>a,d</sup>, Shinji Irie<sup>a,d</sup>, Ryohei Katayama<sup>e</sup>, Hiroshi Shimoda<sup>b,f</sup>, Michiya Matsusaki<sup>a,c,\*</sup>

<sup>a</sup> Joint Research Laboratory (TOPPAN) for Advanced Cell Regulatory Chemistry, Graduate School of Engineering, Osaka University, 2-1 Yamadaoka, Suita, Osaka 565-0871, Japan

<sup>b</sup> Department of Neuroanatomy, Cell Biology and Histology, Graduate School of Medicine, Hirosaki University, 5 Zaifu-cho, Hirosaki, 036-8562, Japan

<sup>c</sup> Department of Applied Chemistry, Graduate School of Engineering, Osaka University, 2-1 Yamadaoka, Suita, Osaka 565-0871, Japan

<sup>d</sup> TOPPAN HOLDINGS INC. TOPPAN Technical Research Institute, 4-2-3, Takanodaiminami, Sugito-cho, Kitakatsushika-gun, Saitama 345-8508, Japan

<sup>e</sup> Division of Experimental Chemotherapy, Cancer Chemotherapy Center, Japanese Foundation for Cancer Research, 3-8-31, Ariake, Koto-ku, Tokyo, 135-8550, Japan

<sup>f</sup> Department of Anatomical Science, Graduate School of Medicine, Hirosaki University, 5 Zaifu-cho, Hirosaki, 036-8562, Japan

## ARTICLE INFO

## Article history:

Received 25 November 2023

Revised 2 July 2024

Accepted 2 July 2024

Available online 6 July 2024

## Key words:

3D cancer-stromal tissue

Collagen microfiber (CMF)

Stiffness

Cancer stem cell marker

## ABSTRACT

The extracellular matrix (ECM) of cancer tissues is rich in dense collagen, contributing to the stiffening of these tissues. Increased stiffness has been reported to promote cancer cell proliferation, invasion, metastasis, and prevent drug delivery. Replicating the structure and mechanical properties of cancer tissue *in vitro* is essential for developing cancer treatment drugs that target these properties. In this study, we recreated specific characteristics of cancer tissue, such as collagen density and high elastic modulus, using a colorectal cancer cell line as a model. Using our original material, collagen microfibers (CMFs), and a constructed three-dimensional (3D) cancer-stromal tissue model, we successfully reproduced an ECM highly similar to *in vivo* conditions. Furthermore, our research demonstrated that cancer stem cell markers expressed in the 3D cancer-stromal tissue model more closely mimic *in vivo* conditions than traditional two-dimensional cell cultures. We also found that CMFs might affect an impact on how cancer cells express these markers. Our 3D CMF-based model holds promise for enhancing our understanding of colorectal cancer and advancing therapeutic approaches.

## Statement of significance

Reproducing the collagen content and stiffness of cancer tissue is crucial in comprehending the properties of cancer and advancing anticancer drug development. Nonetheless, the use of collagen as a scaffold material has posed challenges due to its poor solubility, hindering the replication of a cancer microenvironment. In this study, we have successfully recreated cancer tissue-specific characteristics such as collagen density, stiffness, and the expression of cancer stem cell markers in three-dimensional (3D) colorectal cancer stromal tissue, utilizing a proprietary material known as collagen microfiber (CMF). CMF proves to

**Abbreviations:** 2D, two-dimensional; 3D, three-dimensional; ALDH, aldehyde dehydrogenase; CK20, cytokeratin 20; CLSM, confocal laser scanning microscopy; CMF, collagen microfiber; Col I, collagen type I; DAPI, 4',6-diamidino-2-phenylindole; DEAB, diethylaminobenzaldehyde; DMEM, Dulbecco's Modified Eagle Medium; ECM, extracellular matrix; EGFR, epidermal growth factor receptor; FBS, fetal bovine serum; FPKMs, fragments per kilobase of exon per million mapped fragments; GEF, guanyl-nucleotide exchange factor; GO, gene ontology; GSEA, gene set enrichment analysis; HA, hyaluronic acid; HE, hematoxylin and eosin; LGR5, leucine-rich repeat-containing G-protein-coupled receptor 5; MMP, matrix metalloproteinase; MT, Masson's trichrome; PCA, principal components analysis; PFA, paraformaldehyde; PBS, phosphate buffered saline; TAZ, transcription co-activator with PDZ-binding motif; YAP, Yes-associated protein.

\* Corresponding author at: Department of Applied Chemistry, Graduate School of Engineering, Osaka University, 2-1 Yamadaoka, Suita, Osaka 565-0871, Japan.

E-mail address: [m-matsus@chem.osaka-u.ac.jp](mailto:m-matsus@chem.osaka-u.ac.jp) (M. Matsusaki).

<https://doi.org/10.1016/j.actbio.2024.07.001>

1742-7061/© 2024 The Authors. Published by Elsevier Ltd on behalf of Acta Materialia Inc. This is an open access article under the CC BY-NC-ND license (<http://creativecommons.org/licenses/by-nc-nd/4.0/>)

be an ideal scaffold material for replicating cancer stromal tissue, and these 3D tissues constructed with CMFs hold promise in contributing to our understanding of cancer and the development of therapeutic drugs.

© 2024 The Authors. Published by Elsevier Ltd on behalf of Acta Materialia Inc.  
This is an open access article under the CC BY-NC-ND license  
(<http://creativecommons.org/licenses/by-nc-nd/4.0/>)

## 1. Introduction

Two-dimensional (2D) cell cultures, commonly used as the simplest cancer model, are readily available for human-derived cells and offer superior throughput. However, cells grown in 2D monolayer cultures on rigid plastic substrates do not reflect the cancer microenvironment. They may behave differently in morphology, differentiation, and cell-cell and cell-matrix interactions than cells growing in a three-dimensional (3D) environment such as a living organism [1–4]. Moreover, genetic mutations are likely to occur during the culture process, making it challenging to maintain the original characteristics. For a more precise understanding of the cancer properties and to address issues in tumor therapy, such as drug delivery and chemotherapy resistance, constructing a 3D tissue model that is similar to the living body is necessary.

One of the 3D cancer tissue models is the spheroid. In spheroids, it is possible to generate heterogeneous cancer tissue from a homogeneous cell population. However, spheroids cultured without added scaffold material fail to create an extracellular matrix (ECM) like the cancer microenvironment, thereby limiting the reproduction of cell-stromal interactions and biomechanical properties [5]. In recent years, it has become clear that the characteristics of the environment surrounding the cells, such as hydrophobicity, pore size, fiber diameter, morphology, and molecular crowding, have a marked impact on cell functions [6–10]. Therefore, accurate reproduction of the extracellular environment, such as the structure and density of the ECM, has been emphasized in the construction of tissue models.

Collagen type I (Col I) is the main constituent of the ECM and plays an important role in scaffolds for cell adhesion, mechanical support of tissues and organs, and interactions with other constituents of the ECM or growth factors [11]. Especially in cancer tissues, there is an excessive accumulation of ECM produced by fibroblasts, leading to increased collagen deposition and cross-linking within it. As a result, a cancer stroma primarily composed of Col I and exhibiting a high elastic modulus emerges [12]. In a recent study, control colon tissue showed an elastic modulus of  $0.8 \pm 0.4$  kPa, whereas colon carcinoma tissue showed an elastic modulus of  $2.40 \pm 1.83$  kPa, representing a difference in tissue stiffness of about four-fold [13].

Collagen hydrogels have been used in many studies as scaffolds for 3D cancer cell culture to reproduce the ECM of collagen-rich cancers [14–17]. Although collagen is present in cancer tissue at high concentrations of approximately 20–30 % [18], fabricating collagen hydrogels with high concentrations remains difficult because of their generally poor solubility. In fact, of the studies that have attempted to reproduce cancer tissue using collagen gels, the maximum reported Col I concentration was 0.34 %, resulting in an elastic modulus of 1.2 kPa [19].

More than 10 colorectal cancer stem cell markers have been identified, including CD24, CD29, CD44, CD166, EpCAM, leucine-rich repeat-containing G-protein-coupled receptor 5 (LGR5), and aldehyde dehydrogenase (ALDH) [20]. Cells expressing these markers have the ability to generate clones and recapitulate primary tu-

mors [21]. Subsets of these cancer stem cell markers are also associated with tumor stage, invasion, and metastasis [21]. Cancer stem cells, which are associated with cancer genesis and progression, are promoted in human colorectal cancer by Col I, a process mediated by the  $\alpha 2$  integrin [22]. It has also been reported that cancer tissue stiffness affects the expression of cancer stem cell markers [23], so determining the association between Col I-induced stiffening of tumor tissue and changes in the expression of cancer stem cell markers deserves clinical attention.

We recently reported a novel tissue engineering method using collagen microfibers (CMFs) called “sedimentary culture”. These micro-sized natural Col I with fiber lengths of  $228 \pm 147$   $\mu\text{m}$  and diameters of  $13 \pm 5$   $\mu\text{m}$ , could be used to produce 3D tissue models with high collagen density (up to 20–30 wt%) similar to those *in vivo* [24–27]. In this study, we constructed 3D colorectal cancer-stromal tissue using CMFs to reproduce the histological characteristics of high-density collagen content and mechanical stiffness, which are very similar to those of *in vivo* tissues (Fig. 1). We also examined the expression of cancer stem cell markers and assessed the biological similarity in the constructed 3D cancer-stromal tissue.

## 2. Materials and methods

### 2.1. Cell culture

Human colorectal cancer cell lines HT-29, HCT116 and Colo-320 were purchased from American Type Culture Collection, and HT-115 was purchased from European Collection of Authenticated Cell Cultures. We selected cell lines with different histological types and genetic mutations (Table S1) [28]. These cell lines were maintained in Dulbecco's Modified Eagle Medium (DMEM) (Nacalai Tesque, Kyoto, Japan) supplemented with 10 % fetal bovine serum (FBS) (Thermo Fisher Scientific, Waltham, USA). The patient-derived cell named JC-011 was established from a surgically resected primary ascending colon cancer. The study was conducted in accordance with a protocol approved by the institutional review board (IRB) of Japanese Foundation for Cancer Research (#2013–1093). The patient was male and 50 years old when he received a surgery. After residual tumor pieces are excised from the surgically resected tumor of ascending colon, tumor cells were minced by scalpel and washed 3 times with PBS containing Antibiotic-Antimycotic (Invitrogen, Carlsbad, CA, USA), and enzymatic digested with Collagenase/Dispase with DNase I (Roche, Mannheim, Germany) at 37 °C for 1 hour. After enzymatic digestion, the cells were washed 5–7 times with PBS containing 0.5 % bovine serum albumin and Antibiotic-Antimycotic for to prevent bacterial contamination. Cells were then seeded onto Col I-coated dish in StemPro hESC medium (Invitrogen). Cell stocks were generated after 2 passages, and cells within passages 5–10 were used for experiments. Before subsequent experiments, JC-011 was seeded in Col I-coated dishes and maintained in RPMI-1640 (FUJIFILM Wako, Osaka, Japan) and Ham's F-12 (FUJIFILM Wako) mixed (1:1) medium supplemented with 15 % FBS. Cell cultivation was performed at 37 °C in a humidified atmosphere of 5 % CO<sub>2</sub>.

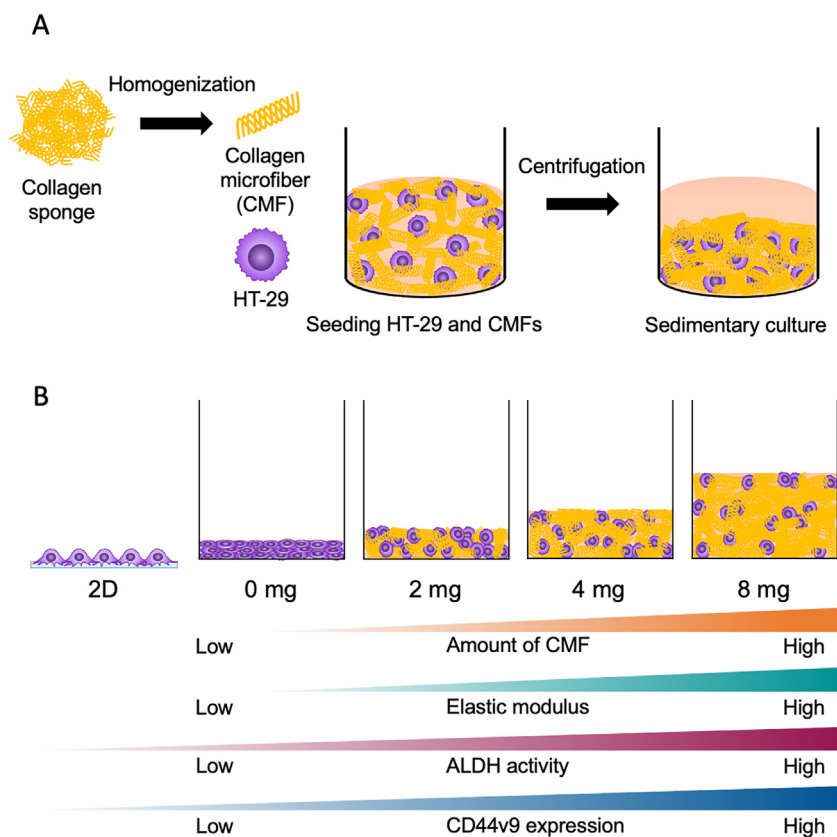


**Fig. 1.** Outline of the present study. (A) Illustration of the construction process for a 3D cancer-stromal tissue using CMFs through sedimentary culture. (B) Overview of the relationship among the amounts of CMFs in the 3D cancer-stromal tissues, the stiffness, and the expression of cancer stem cell markers.

## 2.2. Construction of 3D colorectal cancer-stromal tissue

CMF preparation was performed as described in our previous study [27]. Col I derived from porcine skin was kindly provided by Nippon Ham Foods Ltd., Japan. Briefly, to prepare the CMFs, pieces of collagen sponge were homogenized for 6 min in 10× phosphate buffered saline (PBS) using a homogenizer (VIOLAMO VH-10 homogenizer, S10N-8 G with a diameter of 8 mm and length of 115 mm), and then rinsed with DMEM without FBS by centrifugation at 10,000 rpm for 3 min. Col I powder (Nippi, Tokyo, Japan) was also used in the study of cancer stem cell marker expression. After mixing CMFs and cancer cells, the mixture was put into 24-well plate transwells (0.4 μm porosity, CORNING, NY, USA) to construct 3D cancer-stromal tissue, then the transwells were centrifuged at 1100 g for 15 min. Each 3D cancer-stromal tissue contained  $1.0 \times 10^6$  cancer cells per transwell. The mixtures were cultivated for 7 days in 12 ml/well of DMEM supplemented with 10 % FBS using a 6-well plate (3810-006, Iwaki, Shizuoka, Japan) and self-made adaptors [27]. The medium was changed every 3–4 days.

For 2D culture comparison samples, all colorectal cancer cells were cultured in 6-well plates at  $1.0 \times 10^5$  cells/well for 7 days using 12 ml/well of DMEM supplemented with 10 % FBS, which was the same volume as 3D tissue.

## 2.3. Generation of *in vivo* cancer tissues by xenograft of HT-29 cells on mice

BALB/c nu/nu mice were purchased from CLEA Japan, Inc., Tokyo. In this study, we used 6-week-old female mice that were housed at the Institute for Animal Experiments of Hirosaki University. HT-29 cells were suspended in DMEM without serum at a concentration of  $5.0 \times 10^7$  cells/ml. Two mice received subcuta-

neous injections of 50 μl of the cell suspension ( $2.5 \times 10^6$  HT-29 cells) administered at five positions of their back skin. Seven days post-injection, the formation of *in vivo* cancer tissues generated by HT-29 cells was confirmed by observing skin elevation with a diameter of 3–5 mm. Following euthanasia of the mice, the cancer tissues were carefully excised, with the subcutaneous tissue removed using fine scissors and forceps. The collected tissues were then used for histological analysis and isolation of HT-29 cancer cells as described in 2.4, 2.7 and 2.8, respectively. All procedures for animal experiments followed the “Guide for the Care and Use of Laboratory Animals” issued by the National Institute of Health, and were approved by the Animal Research Committee of Hirosaki University (Approval No. M16021).

## 2.4. Histology and immunohistochemistry

All samples were fixed with 4 % paraformaldehyde (PFA) in PBS. After embedding in paraffin, 5 μm sections were prepared for hematoxylin and eosin (HE) staining, Masson’s trichrome (MT) stain and immunohistochemical staining. The colorectal cancer cells were stained brown using anti-Cytokeratin 20 (CK20) antibody (ab76126, Abcam, Cambridge, UK) or Ki-67 antibody (ab16667, Abcam), which were detected using a horseradish peroxidase (HRP) conjugated goat anti-rabbit IgG (Nichirei Biosciences, Tokyo, Japan) and 3,3’-diaminobenzidine (DAB) substrate solution (DAKO, Denmark A/S, Denmark). Counterstaining was performed using hematoxylin. Photomicrographs were captured by an FL EVOS Automicroscope (Thermo Fisher Scientific).

Double immunostaining was performed using 5 μm-thick paraffin sections. Monoclonal antibody against CD44 variant 9 (CD44v9) (LKG-M001, Cosmo Bio, Tokyo, Japan) was stained brown using HRP conjugated secondary antibody (Nichirei BioSciences) and

DAB substrate solution (DAKO). Rabbit antibody against cytokeratin (ab9377, Abcam) was stained blue using alkaline phosphatase conjugated secondary antibody (Nichirei BioSciences) and Vector Blue substrate (Vector Laboratories, Burlingame, CA, USA). Photomicrographs were captured with a BX-60 microscope (Olympus, Tokyo, Japan).

### 2.5. Cell viability assay

Cell viability in 3D cancer-stromal tissues at days 1, 4, and 7 of culture was examined using the CellTiter-Glo 3D Cell Viability Assay (Promega, WI, USA) according to the manufacturer's protocol. 3D tissues were washed 3 times in PBS and then used for the assay. Luminescence was measured using a Synergy HTX Plate Reader (Agilent Technologies, CA, USA).

### 2.6. Measurement of elastic modulus

Compression tests were performed using an EZ Test (Shimadzu, Kyoto, Japan) with a 5 mm diameter spherical jig at room temperature. The elastic modulus was calculated by determining the slope of the stress-strain curve obtained from the test, as well as the height of the 3D cancer-stromal tissue and the contact area of the test jig with the tissue. The height of the 3D cancer-stromal tissue was measured using digital calipers (Digimatic Caliper CD-15CP, Mitutoyo, Japan). The contact area of the jig was calculated by integrating the strain value in the stress-strain curve.

### 2.7. Immunofluorescence analysis

Whole-mount tissues fixed with 4 % PFA were incubated with mouse anti-YAP-associated protein (YAP) monoclonal antibody (sc-101199, Santa Cruz, Texas, USA) or rabbit anti-Ki-67 monoclonal antibody (Abcam) overnight at 4 °C. After washing with PBS, the tissues were stained with Alexa Fluor 647-conjugated goat anti-mouse IgG (Thermo Fisher Scientific) or Alexa Fluor 647-conjugated goat anti-rabbit IgG (Thermo Fisher Scientific). Nucleus and actin filaments were stained with 4',6-diamidino-2-phenylindole (DAPI) (Thermo Fisher Scientific), and Phalloidin-iFluor 488 (ab176753, Abcam), respectively. It has been reported that the anti-YAP antibody used in this study also reacts with transcription co-activator with PDZ-binding motif (TAZ) [29].

The paraffin sections were stained with anti-human CD44v9 antibody (Cosmo Bio) and Alexa Fluor 647-conjugated goat anti-rat IgG antibody (Thermo Fisher Scientific). Fluorescence images were obtained using an FV3000 microscope (Olympus, Tokyo, Japan).

### 2.8. Collection of cancer cells

To recover the cells, the 2D cultures or 3D cancer stromal-tissues were washed with PBS and incubated in Accumax solution (Nacalai Tesque) at 37 °C for 5 min. After collection, the cells were washed with PBS and incubated in 2 mg/ml collagenase from *Clostridium histolyticum* (type I, Sigma-Aldrich, St. Louis, USA) in PBS at 37 °C for 15 min. Cancer cells from *in vivo* tissues were recovered using a Tumor Dissociation Kit (Miltenyi Biotec, Bergisch Gladbach, Germany) according to the manufacturer's protocol. Single cells were prepared by passing them through 70 µm and 40 µm nylon mesh filters.

### 2.9. FACS analysis and sorting of cancer cells

Collected cancer cells were blocked with 10 % FBS in PBS for 30 min on ice and then fluorescence immunostained using the antibodies listed in Table S2. Only in the case of using anti-LGR5 antibody, cancer cells were fixed in 4 % PFA before antibody treatment.

Samples were passed through a 30 µm nylon mesh filter and then analyzed in BD FACSVerser or BD FACSMelody or sorted in BD FACSAriaII (Becton Dickinson, Franklin Lakes, USA). Data were analyzed with FlowJo software.

### 2.10. RNA-sequencing and data analysis

RNA-sequencing was performed by the Genome Information Research Center (Research Institute for Microbial Disease, Osaka University). P4 and P5 populations were sorted according to CD44 and CD44v9 expression in cells collected from 2D culture and 3D cancer-stromal tissue using FACS (Fig. S1). Total RNA was extracted using an miRNeasy Micro Kit (QIAGEN, Venlo, Netherlands). Each cDNA was generated using a Clontech SMART-Seq HT Kit (Takara Clontech, Mountain View, USA). Each library was prepared using a Nextera XT DNA Library Prep Kit (Illumina, San Diego, USA) according to the manufacturer's instructions. Whole transcriptome sequencing was performed to the pool of libraries using an Illumina HiSeq 2500 platform in a 75-base single-end mode. Sequence reads were mapped to the human reference genome sequence (hg19) using TopHat ver. 2.0.13 in combination with Bowtie2 ver. 2.2.3 and SAMtools ver. 1.0. The number of fragments per kilobase of exon per million mapped fragments (FPKMs) was calculated using Cufflinks ver. 2.2.1. Differential expression and pathway analysis of the RNA sequence data were performed using iDEP (<http://ge-lab.org/idep/>) [30].

### 2.11. ALDH assay

The detection of ALDH activity was performed using AldeRed ALDH Detection Assay (Merck Millipore, Darmstadt, Germany) following the manufacturer's protocol [31]. Samples were passed through a 30 µm nylon mesh filter and then analyzed in BD FACSMelody (Becton Dickinson, Franklin Lakes, USA). Data were analyzed with FlowJo software. Diethylaminobenzaldehyde (DEAB), an ALDH inhibitor, was used to treat cells for defining the gated regions.

### 2.12. Statistical analysis

All data are expressed as mean values with their corresponding standard deviations. Differences in the mean values were assessed using a two-tailed Student's *t*-test, and *p*-values less than 0.05 were considered statistically significant.

## 3. Results

### 3.1. 3D colorectal cancer-stromal tissue construction and its characterization

A 3D colorectal cancer-stromal tissue consisting of CMFs and HT-29 cells was constructed. To mimic the ECM density of colorectal cancer tissue *in vivo*, the cell number for the tissues was fixed at  $1.0 \times 10^6$  cells and the amount of CMF was adjusted from 0 to 8 mg. Adding more than 8 mg of CMFs to 3D tissue was technically challenging. The morphology and collagen distribution of the constructed tissues were examined using HE and MT staining (Fig. 2A and S2). HE- and MT-stained images revealed that 3D cancer-stromal tissues, prepared with the addition of CMFs, exhibited a high density of collagen, and the tissue thickness increased in a CMF amount-dependent manner. Furthermore, the immunohistochemistry images of CK20, a type of keratin expressed in colorectal cancer tissue, showed that HT-29 cells were distributed throughout the 3D cancer-stromal tissues (Fig. 2A). The 3D cancer-stromal tissues maintained good cell viability,  $120.01 \pm 16.45$  % at day 4 and  $176.10 \pm 7.62$  % at day 7 (Fig. 2B).

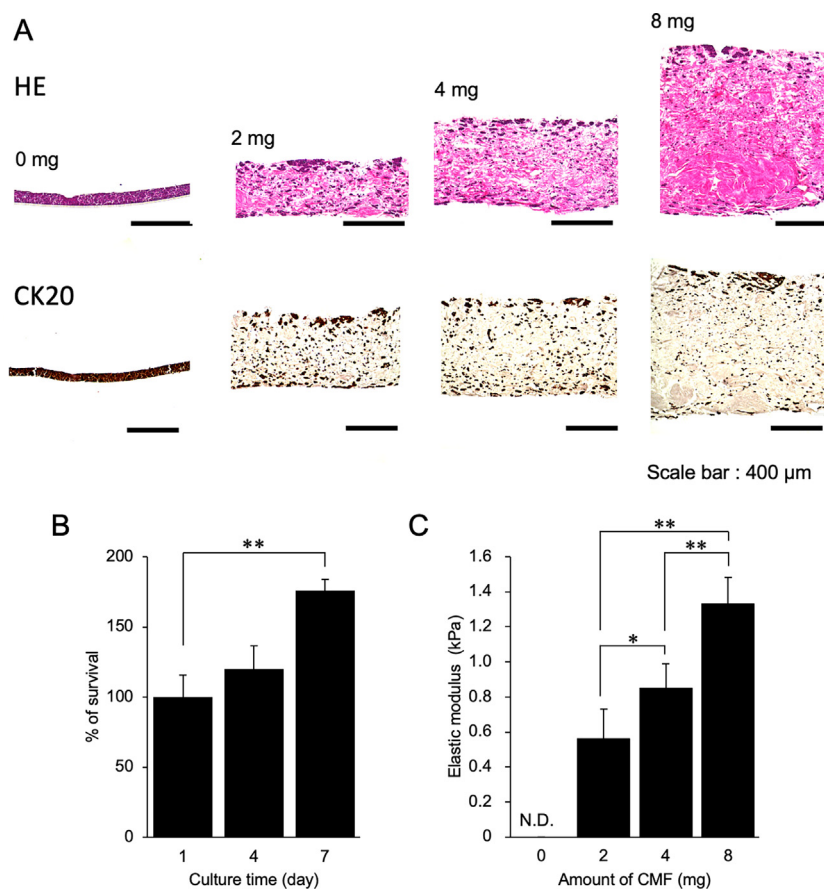


**Fig. 2.** Morphological characteristics of the 3D cancer-stromal tissues. (A) HE staining and immunohistochemical staining of CK20 in 3D cancer-stromal tissue with or without various amounts of CMFs after 7 days of culture. (B) Cell viability of 3D cancer-stromal tissues on days 1, 4, and 7, and presented as relative cell viability compared to day 1. (C) Elastic modulus of 3D cancer-stromal tissues evaluated using a compression test method. Each column represents the means  $\pm$  standard deviations (SD) of three independent tissues. N. D. means not detected. \*  $p < 0.05$ , \*\*  $p < 0.005$ .

The mechanical properties of fabricated 3D cancer-stromal tissues were measured using compression test methods and the elastic modulus was calculated (Fig. 2C). The tissue containing 2 mg of CMFs exhibited an elastic modulus of  $0.56 \pm 0.17$  kPa, whereas the tissue containing 8 mg of CMFs showed  $1.33 \pm 0.15$  kPa, indicating that the elastic modulus of 3D cancer-stromal tissue increases in a CMF amount-dependent manner.

### 3.2. Effect of CMF amount on YAP/TAZ expression and proliferative activities of colorectal cancer cells in 3D cancer-stromal tissues

YAP/TAZ, which functions as an effector of the Hippo pathway, is a mechanotransducer and its activity is necessary for tumor development and progression [32]. To investigate whether mechanical stimuli resulting from increased ECM stiffness are transmitted via YAP/TAZ, we examined YAP/TAZ expression in HT-29 cells in the 3D cancer-stromal tissues (Fig. 3A). In tissues without added CMFs, the red signals indicating the expression of YAP/TAZ were localized to the cytoplasm. However, with increasing amounts of CMFs in the 3D cancer-stromal tissues, the expression of YAP/TAZ migrated to the nucleus, and the red signals localized to the nucleus were significantly increased to  $15.8 \pm 3.7$  % in the tissue prepared with 8 mg of CMFs (Fig. 3B). In addition, HT-29 cells in which YAP/TAZ was activated, showed an enhancement of phalloidin staining signals indicating F-actin. Analysis of YAP/TAZ immunofluorescence staining images indicated that YAP/TAZ activation was dependent on tissue stiffness, which correlated to the increased amount of CMF.

Next, we monitored the expression of the nuclear protein Ki-67 [33], which is used to evaluate cell proliferative ability and is a clinically useful biomarker for cancer subtype classification (Fig. 3C). The percentage of HT-29 cells expressing Ki-67 was highest in 3D cancer-stromal tissues prepared with 8 mg of CMFs at  $52.8 \pm 20.9$ % (Fig. 3D), indicating that the number of HT-29 cells expressing Ki-67 in 3D cancer-stromal tissues increases in a CMF amount-dependent manner. In addition, cells expressing Ki-67 were identified inside the 3D cancer-stromal tissue with 8 mg of CMFs (Fig. S3A). There was no significant difference in the localization of Ki-67 positive cells between the surface and internal areas of the 3D tissue (Fig. S3B). These results provide evidence that YAP/TAZ-mediated signal transduction and cell proliferation as indicated by Ki-67 are activated in 3D cancer-stromal tissues.

### 3.3. Effects on gene expression

As YAP/TAZ and Ki-67 were activated in the 3D cancer-stromal tissues, it was expected that the 3D-organization using CMFs would also affect the expression of various other genes. To investigate this, we performed RNA sequencing to analyze the transcriptome profiles of cells recovered from 2D cultures and 3D cancer-stromal tissues prepared with 8 mg of CMFs, with a particular focus on markers related to cancer stemness, which can be influenced by the culture dimension.

CD44 and CD44v9 were used as cancer stem cell markers for cell recovery. CD44, one of the cell adhesion molecules that adheres to ECM including hyaluronic acid (HA), is known to play a pivotal role in regulating cancer stemness and is involved in tumor

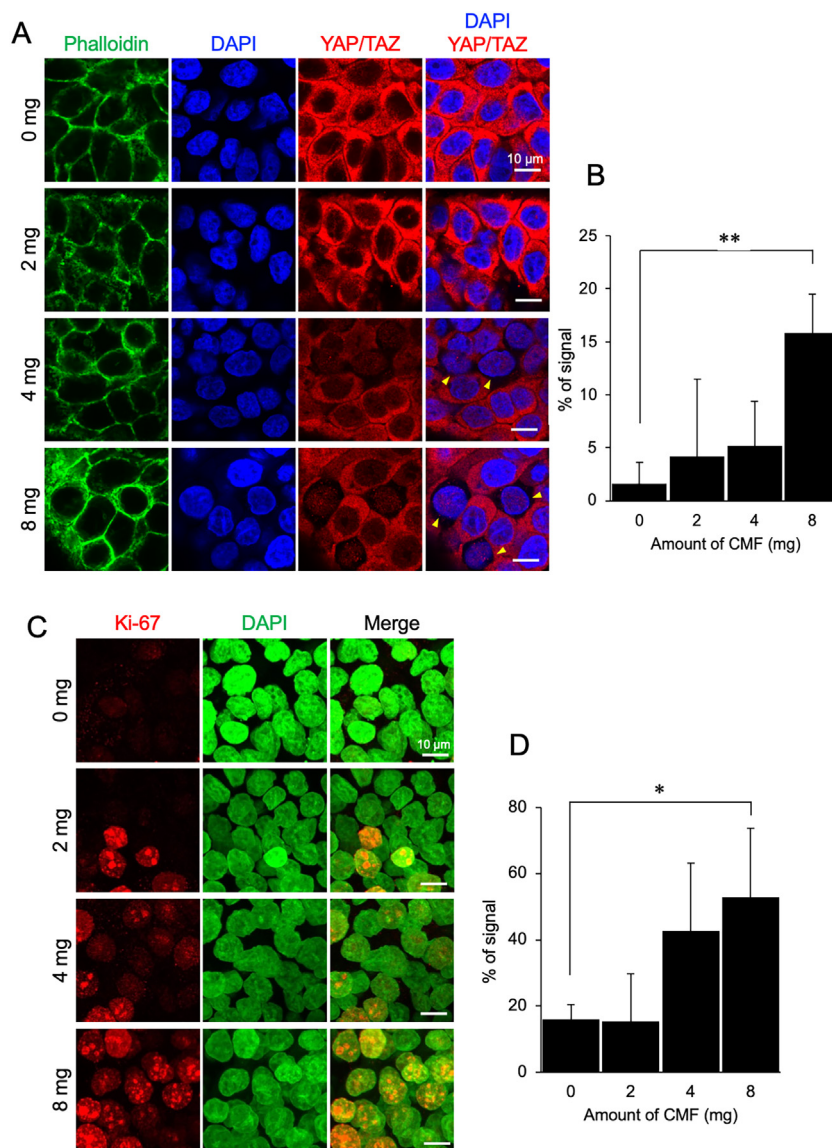


**Fig. 3.** YAP/TAZ and Ki-67 activity in the 3D cancer-stromal tissues. (A) Fluorescence images showing the YAP/TAZ signals. The 3D cancer-stromal tissues were stained with anti-YAP/TAZ (red) antibody, DAPI (blue) and phalloidin (green), respectively, and observed by confocal laser scanning microscopy (CLSM). Yellow arrowheads indicate YAP/TAZ signals localized to the nucleus. Scale bars represent 10  $\mu$ m. (B) Quantitative analysis of activated TAP/TAZ signaling. The graph shows the percentage of YAP/TAZ localized to the nucleus relative to the total number of cell nuclei. Each column represents the means  $\pm$  SD of three or four independent tissues. \*\*  $p < 0.005$ . (C) Fluorescence images of the Ki-67 signals. The tissues were stained with anti-Ki-67 (red) antibody and DAPI (green), respectively, and observed by CLSM. Scale bars represent 10  $\mu$ m. (D) Quantitative analysis of activated Ki-67 signaling. The graph shows the percentage of Ki-67 expressed in the nucleus relative to the total number of cell nuclei. Each column represents the means  $\pm$  SD of three independent tissues. \*  $p < 0.05$ . (For interpretation of the references to color in this figure legend, the reader is referred to the web version of this article.)

cell invasion and metastasis [34–36]. CD44v9, a variant isoform of CD44, has been implicated in hematogenous metastasis [37–39]. Furthermore, CD44<sup>+</sup>/CD44v9<sup>+</sup> colorectal cancer cells have much stronger colony-forming and tumor mass-forming abilities and resistance to anticancer drugs, indicating that CD44 and CD44v9 are important factors for colorectal cancer [40]. Using these cancer stem cell markers as indicators for FACS sorting, we recovered CD44<sup>+</sup>/CD44v9<sup>-</sup> (P5 population) and CD44<sup>+</sup>/CD44v9<sup>+</sup> (P4 population) cells from HT-29 cells in 2D cultures and 3D tissues, and performed gene expression comparisons (Fig. S1).

A principal components analysis (PCA), represented by first and second principal components, was performed to assess the similarity of gene expression to 2D culture and 3D cancer-stromal tissue (Fig. 4A). The CD44<sup>+</sup>/CD44v9<sup>+</sup> plots of 2D culture and 3D cancer-stromal tissue occupied close positions. However, clear dif-

ferences were observed between CD44<sup>+</sup>/CD44v9<sup>-</sup> cells in the 2D cultures and the other three fractions. In particular, the similarity in gene expression was low between the 2D cultures and the 3D cancer-stromal tissues, despite the cell populations exhibiting the same CD44<sup>+</sup>/CD44v9<sup>-</sup> expression type. Pathway gene set enrichment analysis (GSEA) for Gene Ontology (GO) molecular function was then conducted using the largest percentage of the population in each culture system: the CD44<sup>+</sup>/CD44v9<sup>+</sup> cells of 3D cancer-stromal tissue (3D P4) and the CD44<sup>+</sup>/CD44v9<sup>-</sup> cells of 2D culture (2D P5). This analysis aimed to identify molecular functions that were promoted in the 3D cancer-stromal tissues (Fig. 4B). It revealed that the expression of genes involved in pathways associated with cell proliferation leading to accelerated cancer progression, such as Ras and Rho guanyl-nucleotide exchange factor (GEF), were up-regulated in the CD44<sup>+</sup>/CD44v9<sup>+</sup> cells of 3D

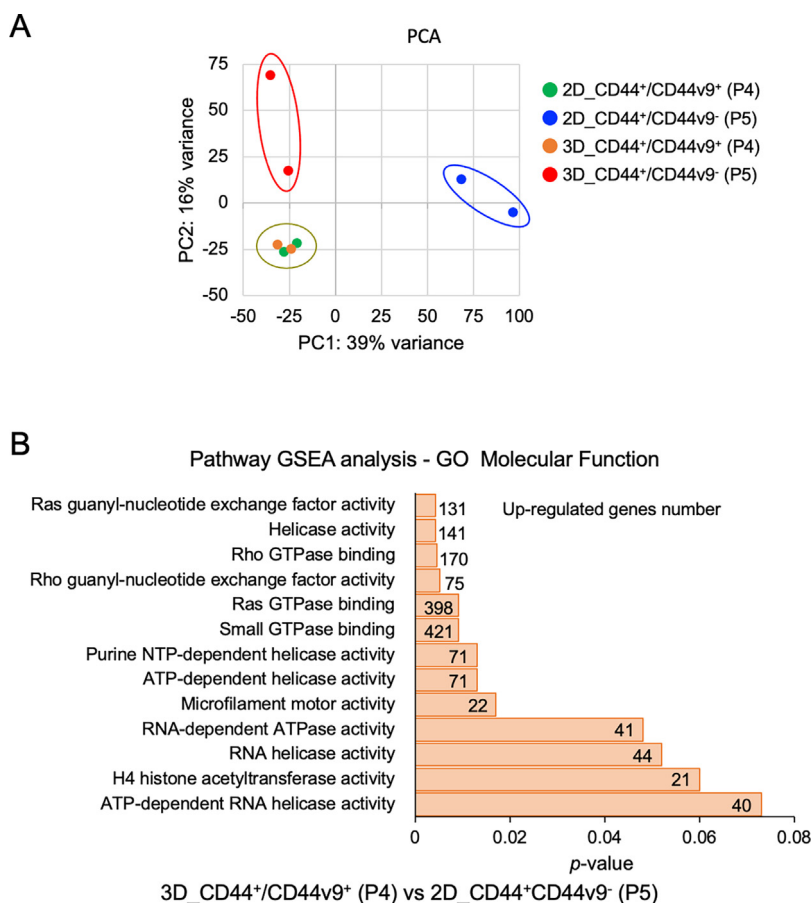


**Fig. 4.** RNA-sequencing analysis of 3D cancer-stromal tissues compared to 2D cultures. (A) Principal component analysis (PCA) of P4 and P5 populations in 2D cultures and P4 and P5 populations in 3D cancer-stromal tissue. (B) Significantly up-regulated genes in P4 population of 3D cancer-stromal tissue compared to P5 population of 2D culture using pathway GSEA analysis for the GO molecular function.

cancer-stromal tissues compared to the CD44<sup>+</sup>/CD44v9<sup>-</sup> cells of 2D cultures.

### 3.4. Similarity of 3D cancer-stromal tissue to *in vivo* tissue

To verify the biological similarity of 3D cancer-stromal tissues constructed with CMFs, protein expression levels of CD44 and CD44v9 were analyzed in comparison to *in vivo* tissue. We employed xenografts, generally used as a mouse tumor model in many studies, as the *in vivo* tissues condition. HE-stained images indicated that a tumor mass was established at 7 days post-injection (Fig. S4A). Furthermore, immunohistochemical staining images depicted the localization of numerous CD44v9-positive cells within the tumor mass (Fig. S4B). Immunofluorescence staining images showed CD44v9-positive signals in both 3D cancer-stromal tissues and *in vivo* tissues (Fig. 5A). In addition, FACS plots of CD44 and CD44v9 were fractionated quadratically (Fig. 5A), showing the percentage of HT-29 cells in each fraction (Fig. 5B). The *in vivo* tissue was mostly composed of CD44<sup>+</sup>/CD44v9<sup>+</sup> cells. On the other hand, in 2D cultured cells, the CD44<sup>+</sup>/CD44v9<sup>+</sup> and CD44<sup>+</sup>/CD44v9<sup>-</sup> cells accounted for  $22.1 \pm 14.3$  % and  $75.6 \pm 15.9$  %, respectively. In the 3D cancer-stromal tissue, CD44<sup>+</sup>/CD44v9<sup>+</sup> cells accounted for  $63.3 \pm 25.3$  % of the cells, albeit less than in the *in vivo* tissues, while CD44<sup>+</sup>/CD44v9<sup>-</sup> cells accounted for  $34 \pm 23.1$  %. These results revealed that the expression of CD44 and CD44v9 in the 3D cancer-stromal tissues more closely resembles that of *in vivo* tissues compared to 2D cultures. The expression of CD44v9 in HT-29 cells approached levels observed in *in vivo* tissues through 3D-organization using CMFs,

suggesting the potential involvement of CMF scaffolds and three-dimensionalization.

In the 3D cancer-stromal tissue, CD44<sup>+</sup>/CD44v9<sup>+</sup> cells increased with increasing days of culture, but decreased in 2D culture (Fig. 5C). This indicates that cancer stem cells increased in the 3D cancer-stromal tissue with 7 days of culture.

In addition, we measured ALDH activity in HT-29 derived from the 3D cancer-stromal tissues and the *in vivo* tissues (Fig. S5). The ALDH activity was relatively high in HT-29 cells derived from the 3D cancer-stromal tissues ( $8.99 \pm 3.4$ ) and the *in vivo* tissues ( $6.59 \pm 5.07$ ) though not significantly different. These results indicate that the ALDH activity in 3D cancer-stromal tissues is similar to that in *in vivo* tissues. Thus, cancer cells in 3D cancer-stromal tissues closely resemble cancer cells in tumor tissues generated *in vivo*, as evidenced by the expression of cancer stem cell markers.

### 3.5. Comparative analysis of cancer stem cell marker expression in the 3D cancer-stromal tissue versus the 2D culture

Finally, we constructed a 3D cancer-stromal tissue with not only HT-29 cells but also other human-derived colorectal cancer cell lines Colo-320, HT-115, HCT116 and cancer patient-derived cell JC-011 and examined the expression of various cancer stem cell markers (Fig. 6 and S6–10). CD44v9 expression was significantly increased in all cell types in the 3D cancer-stromal tissue. E-cadherin expression also showed an increasing trend, although some cell types did not show significant differences. In addition, CD166 and epidermal growth factor receptor (EGFR) expression were also sig-



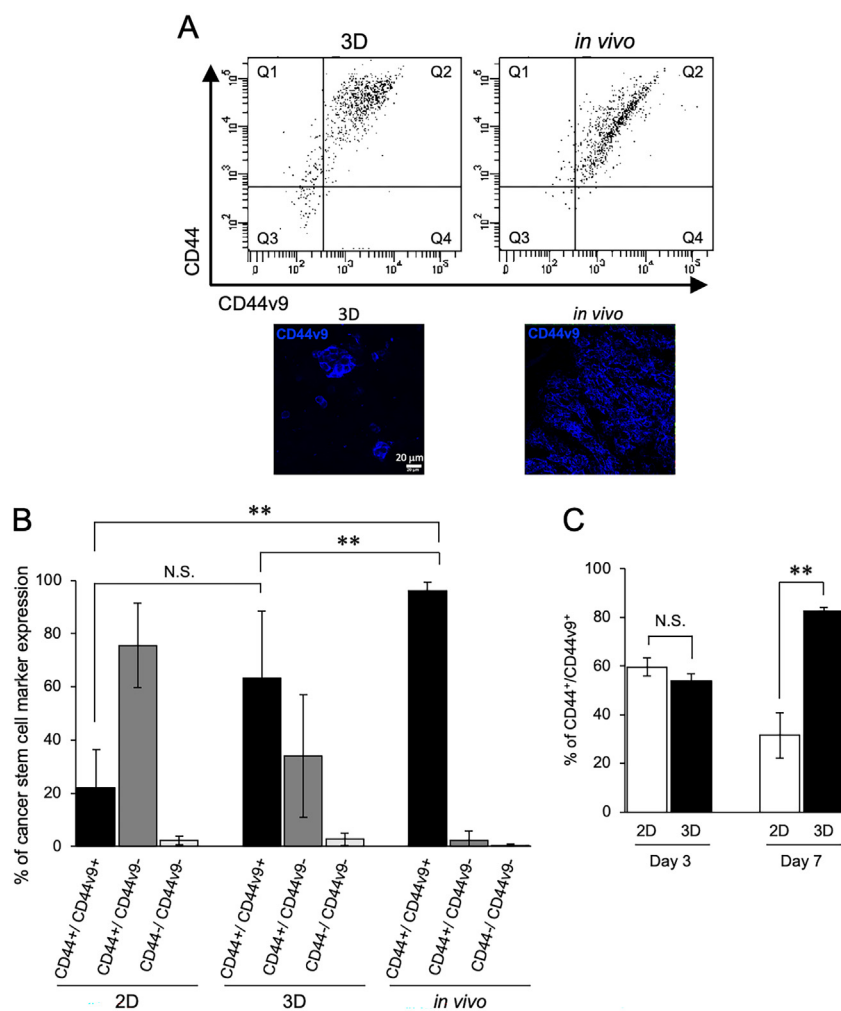


**Fig. 5.** Comparison of expression of cancer stem cell markers CD44 and CD44v9. (A) Expression plots of CD44 and CD44v9 in 3D cancer-stromal tissues and *in vivo* tissues along with fluorescence imaging of tissues stained with anti-CD44v9 antibody. Q1: CD44<sup>-</sup>/CD44v9<sup>-</sup>, Q2: CD44<sup>+</sup>/CD44v9<sup>+</sup>, Q3: CD44<sup>-</sup>/CD44v9<sup>+</sup>, Q4: CD44<sup>+</sup>/CD44v9<sup>-</sup>. (B) Expression analysis of CD44 and CD44v9 in 2D cultures, 3D cancer-stromal and *in vivo* tissues. Each column represents the means  $\pm$  SD. "N. S." means non-significant difference. \*\*  $p < 0.005$ . (C) Time-dependent changes in the percentage of CD44<sup>+</sup>/CD44v9<sup>+</sup> cells in 2D culture and 3D cancer-stromal tissue. Each column represents the means  $\pm$  SD. "N. S." means non-significant difference. \*\*  $p < 0.005$ .

nificantly altered, and LGR5 expression was significantly different only in patient-derived cell JC-011. The HT-115 cells exhibited the highest number of up-regulated cancer stem cell markers (7 markers), while the HT-29 cells displayed the lowest (3 markers). Conversely, the HT-29 cells showed the highest number of down-regulated cancer stem cell markers (5 markers), with the HCT116 cells exhibiting the lowest (1 marker). Significant expression changes in the highest number of cancer stem cell markers (9 markers) were observed in HT-115 cells. The histogram of JC-011 showed a contrasting histogram shape unlike other cell lines, mainly in the expression of CD44 and CD44v9 (Fig. S6-S10). Furthermore, ALDH activity was significantly increased in Colo-320, HCT116 and HT-29 cells compared to 2D cultures (Fig. 7) but no significant changes were observed in JC-011. ALDH activity was compared in HT-29 cells in 2D culture, 3D cancer-stromal tissue, and *in vivo* tissue. Significantly lower ALDH activity was observed in 2D culture, whereas comparable activity was observed in 3D cancer-stromal and *in vivo* tissues (Fig. S5 and 7B). Three-dimensional organization of cancer cell lines using CMFs led to changes in the expression of cancer stem cell markers, suggesting that fibrous collagen and three-dimensionalization may have an impact on the expression of cancer stemness of colorectal cancer cells.

#### 4. Discussion

In this study, we selected CMFs as the scaffold material to construct 3D colorectal cancer-stromal tissue, aiming to reproduce the fibrous collagen, tissue stiffness and cellular characteristics observed in cancer tissue. Using this technique, we were able to create 3D cancer-stromal tissue that accurately mimicked the morphology and density of collagen fibers found in cancer tissue, replicating its histological features.

Colorectal cancer tissue has been reported to exhibit a stiffness of  $2.40 \pm 1.83$  kPa [13]. In our study, we were able to construct a 3D cancer-stromal tissue with a stiffness of 1.4 kPa by using 8 mg of CMFs. The 3D cancer-stromal tissue closely approximated the native mechanical properties of tumor tissue by incorporating micro-sized fibers of Col I. However, the elastic modulus in the 3D cancer-stromal tissues was found to be lower than in the *in vivo* cancer tissues. *In vivo*, tumor tissue stiffens due to increased deposition of ECM, reduced matrix metalloproteinase (MMP)-mediated matrix degradation, and collagen cross-linking. In addition, the tumor mass of colorectal cancer contains not only the ECM and cancer cells, but also fibroblasts, immune cells, and vascular network structures. Consequently, the stiffness of the ECM affects not only cancer cells but also fibroblasts [41]. Increased ECM stiffness leads

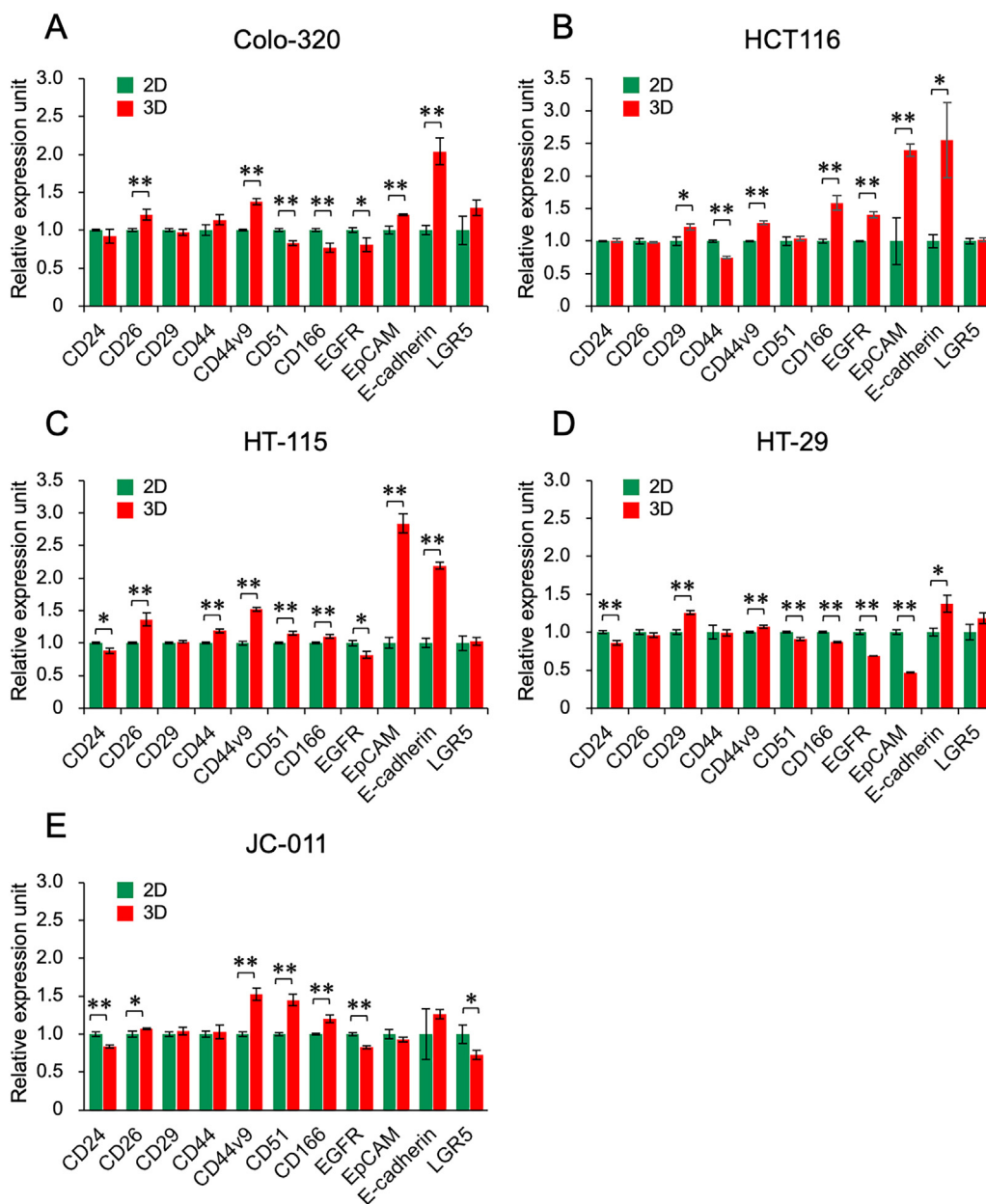


**Fig. 6.** Relative expression levels of cancer stem cell markers in 3D cancer-stromal tissues compared to 2D culture. Expression of CD24, CD26, CD29, CD44 CD44v9, CD51, CD166, EGFR, EpCAM, E-cadherin, LGR5 in Colo-320 (A), HCT116 (B), HT-115 (C), HT-29 (D) and JC-011 (E) cells was measured using FACS. Each column represents the means  $\pm$  SD of three independent tissues. \*  $p < 0.05$ , \*\*  $p < 0.005$ .

to inhibition of IL-1 $\beta$  and IL-1 $\beta$ -responsive inflammatory genes in fibroblasts, resulting in decreased MMP expression and a further increase in ECM stiffness [42]. The 3D cancer-stromal tissue constructed in this study solely comprises CMFs and cancer cells, thus its stiffness was found to be lower than in *in vivo* cancer tissue. In the future, achieving stiffness more similar to solid tumors may be feasible by incorporating fibroblasts and integrating vascular network structures into the 3D cancer-stromal tissues.

Another important marker to examine is YAP/TAZ which is activated in various human cancers and promotes tumor initiation, progression, and metastasis. Moreover, activation of YAP/TAZ is associated with poor prognosis [43–46]. The activity of YAP/TAZ is generally regulated by the stiffness of the ECM and its activation may promote cancer cell proliferation and survival [47]. Indeed, YAP/TAZ promotes tumor growth by cell cycle progression and by transactivating anti-apoptosis-related genes [48,49]. However, it is

inhibited when the cell adhesion area is restricted on the stiff substrate in 2D culture, suggesting that not only ECM stiffness but also cell extension is involved in YAP/TAZ activation [50]. In the 3D cancer-stromal tissue, the level of CMF was found to be dependent on the tissue stiffness, triggering actin activation, which in turn led to the activation of YAP/TAZ and Ki-67, in the same manner as *in vivo*.

Furthermore, GEF is involved in many signaling pathways, especially those related to cell proliferation [51]. GEF activates signaling pathways related to Ras and Rho through the activation of GTPases. Ras and Rho are associated with cancer progression, metastasis, and prognosis [52,53]. In addition, *in vivo* cancer cells respond to the mechanical microenvironment through Rho signaling, such as cell proliferation and metastasis [54]. In the present study, 3D-organized HT-29 cells up-regulated the gene expression related to Ras and Rho signaling pathways compared to 2D cul-

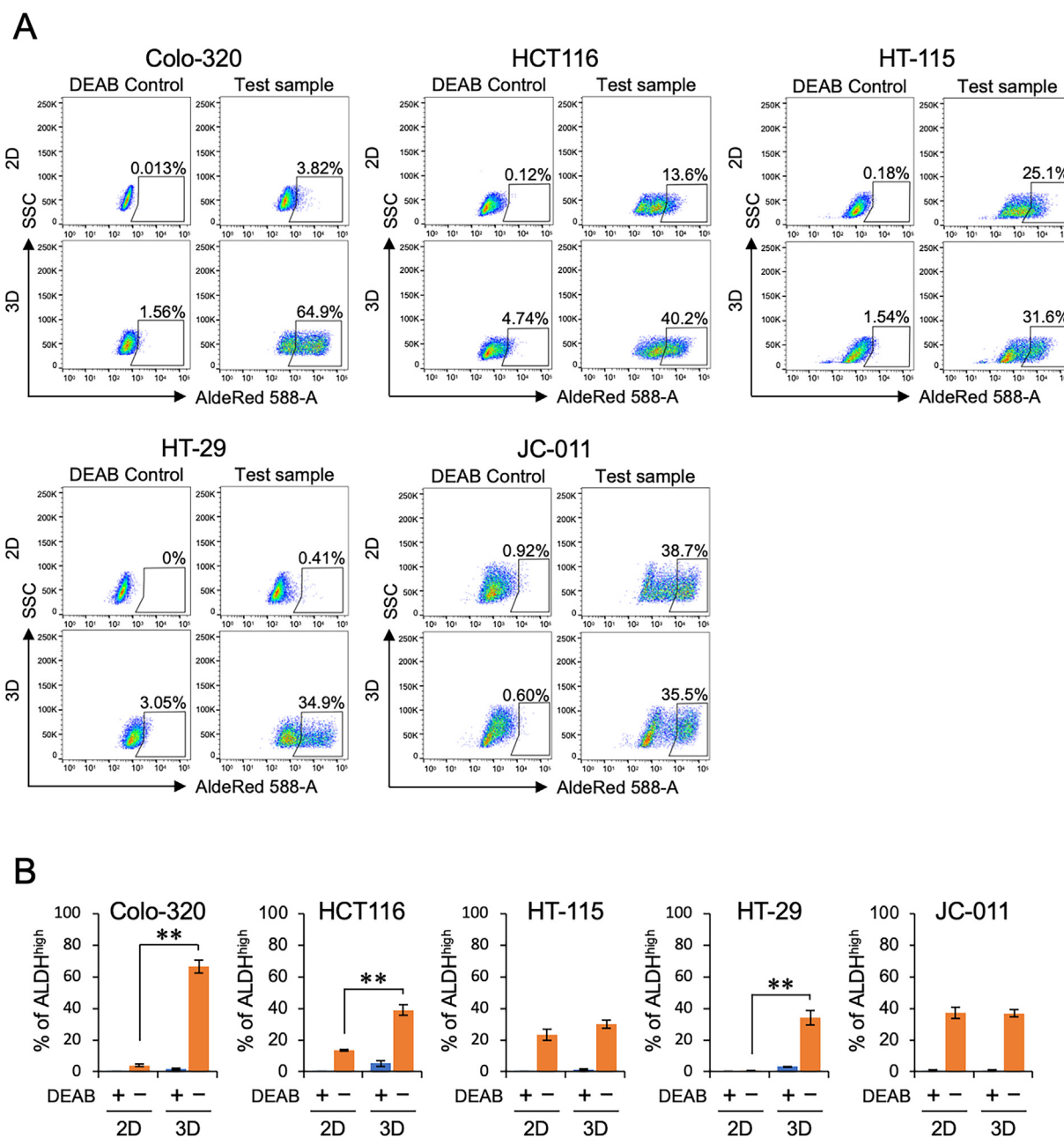


**Fig. 7.** ALDH activity in 2D cultures and 3D cancer-stromal tissues. (A) FACS plots of ALDH activity in Colo-320, HCT116, HT-115, HT-29 and JC-011 cells. (B) The graph shows the percentage of ALDH-positive cells in each examined cell type. Each column represents the means  $\pm$  SD of three independent tissues. \*  $p < 0.05$ . \*\*  $p < 0.005$ .

ture. This observed increase in gene expression could potentially be attributed to the generation of a cancer microenvironment-like condition for cancer cells through the use of CMFs.

A previous study found that there is a suitable stiffness for the expression of cancer stem cell markers, a matrix stiffness of 25 kPa being optimal for the colorectal cancer cell line HCT116 [55]. The substrates used in 2D cultures have a stiffness of 100,000 kPa. In addition, monolayer cultures cannot develop a tumor microenvironment and reproduce the cell-matrix interactions and mechanical effects found in tumor tissues. The presence of Col I is another factor that promotes an increase in cancer stem cells [22]. The 3D cancer-stromal tissue is rich in Col I, the primary component of the tumor stroma, creating a physical and biochemical environment that closely resembles cancer tissue, in contrast to 2D culture. Consequently, the 3D cancer-stromal tissue recapitulated cell-

stromal interactions and mechanical stimuli, potentially leading to a stronger resemblance to *in vivo* tissue compared to 2D culture, particularly in terms of CD44 and CD44v9 expression.

Analysis of CD44 and CD44v9 expression levels revealed the presence of two populations in HT-29 cells: a CD44<sup>+</sup>/CD44v9<sup>+</sup> population and a CD44<sup>+</sup>/CD44v9<sup>-</sup> population. Interestingly, the CD44<sup>+</sup>/CD44v9<sup>+</sup> population increased in a time-dependent manner in 3D cancer-stromal tissue, but decreased in 2D cultures. CD44<sup>+</sup>/CD44v9<sup>+</sup> cancer cells have been reported to have significantly higher tumor mass formation capacity and drug resistance [40]. Taken together, cancer cells cultured in 3D cancer-stromal tissue may allow them to progress toward enhanced cancer stemness levels.

It has been shown that ECM stiffness also regulates cancer stem cell properties in colorectal cancer [23]. In this experiment, we

conducted FACS analysis to examine the expression of 12 cancer stem cell markers. CD44v9 was significant increased in all colorectal cancer cell types used to generate the 3D cancer-stromal tissue. CD44v9 contributes to cancer survival by promoting cystine uptake and increasing oxidative stress resistance [40]. The interaction of CD44 with its ligands such as HA, collagens and MMPs, contributes to migration and invasion processes in cancer [56]. Furthermore, collagen degradation has an important role in inhibiting tumor invasion and migration. Suwannakul et al. reported that CD44v9 knockdown inhibited cholangiocarcinoma invasion and migration via HA suppression and collagen replacement [57]. These reports support our finding that CD44v9 expression was higher in the 3D cancer-stromal tissue than in 2D cultures for all cell lines. The histogram of JC-011 was divergent when compared to histograms of other cultured cell lines, especially in the expression of CD44 and CD44v9. These results may be attributed to the fact that JC-011 is a patient-derived cancer cell line. Cancer tissues are highly heterogeneous, and heterogeneity exists even within the same patient's tumor tissue. This may have led to differences in responsiveness to CMF-based 3D-organization, resulting in variations in the expression of CD44 and CD44v9. LGR5 expression was variable only in JC-011, a patient-derived cell. One of the problems with cancer cell lines is the loss of phenotypic and genetic heterogeneity found in the original tumor [58]. The expression of LGR5 may be affected by these factors. E-cadherin is an adhesion molecule that, when lost, has been proposed to initiate invasion and metastasis to surrounding tissues [59,60]. On the other hand, recent studies have reported that E-cadherin expression is required for metastasis in breast cancer [61]. Moreover, in colorectal cancer stem cells, E-cadherin-positive cells have been shown to exhibit higher tumor growth potential *in vivo* [62]. In the 3D cancer-stromal tissue, increased E-cadherin expression was observed. Although it remains to be discussed whether the expression of E-cadherin in 3D cancer-stromal tissue can reproduce phenomena such as metastasis and cell proliferation in *in vivo* cancer tissue, this 3D tissue may hold promise as a tool for cancer research. Finally, the 3D-organization of cancer cells using CMFs demonstrated significant variation in the expression of various cancer stem cell markers, suggesting the importance of collagen fibers for colorectal cancer cells. However, additional studies using patient-derived cells will be necessary to further elucidate the relationship between CMFs, tissue stiffness and cancer stem cell markers. These studies will also be essential to demonstrate the effectiveness and robustness of 3D colorectal cancer-stromal tissues.

## 5. Conclusion

We reported that 3D cancer-stromal tissue produced with CMFs reproduced collagen density, stiffness, and expression of cancer stem cell markers similar to *in vivo* conditions. In cancer therapy, the deposition of Col I and the associated stiffening of tumor tissue may affect the efficacy of therapeutic agents. Our findings showed that the collagen fiber content and mechanical stiffness in 3D cancer-stromal can be modulated by micro-sized natural Col I. This 3D tissue may lead to new applications in the study of complex cancer progression mechanisms and the development of therapeutic drugs. However, in this study, we mainly used cell lines to validate 3D colorectal cancer-stromal tissues. Therefore, we have not fully demonstrated how faithfully we can replicate *in vivo* conditions. For potential applications as *in vivo* models, it is necessary to enhance the *in vivo* similarity of the model tissue by adding fibroblasts and capillary network structures to the stromal tissue, and to increase the number of studies using patient-derived cancer cells. We expect that our 3D colorectal cancer-stromal tissue using CMFs will contribute to a better understanding of colorectal cancer and to the advancement of its therapy.

## Declaration of competing interest

The authors declare that they have no known competing financial interests or personal relationships that could have appeared to influence the work reported in this paper.

## CRedit authorship contribution statement

**Naoko Sasaki:** Writing – review & editing, Writing – original draft, Visualization, Validation, Project administration, Methodology, Investigation. **Yoshiya Asano:** Writing – review & editing, Writing – original draft, Validation, Resources, Methodology, Investigation. **Yukiko Sorayama:** Visualization, Validation, Investigation. **Chihiro Kamimura:** Visualization, Validation, Investigation. **Shiro Kitano:** Funding acquisition, Conceptualization. **Shinji Irie:** Writing – review & editing, Visualization, Methodology. **Ryohei Katayama:** Writing – review & editing, Writing – original draft, Supervision, Resources. **Hiroshi Shimoda:** Writing – review & editing, Writing – original draft, Supervision, Resources. **Michiya Matsusaki:** Writing – review & editing, Supervision, Resources, Project administration, Methodology, Funding acquisition, Data curation, Conceptualization.

## Acknowledgements

We thank NH Foods Ltd. for their kind donation of porcine skin-driven type I collagen sponges. We thank Dr. K. Sumiyoshi for helpful suggestions and technical support. This research was supported by Grant-in-Aid for Scientific Research (A) (20H00665).

## Supplementary materials

Supplementary material associated with this article can be found, in the online version, at [doi:10.1016/j.actbio.2024.07.001](https://doi.org/10.1016/j.actbio.2024.07.001).

## References

- [1] A. Birgersdotter, R. Sandberg, I. Ernberg, Gene expression perturbation *in vitro* – a growing case for three-dimensional (3D) culture systems, *Semin. Cancer Biol.* 15 (2005) 405–412, doi:[10.1016/j.semcancer.2005.06.009](https://doi.org/10.1016/j.semcancer.2005.06.009).
- [2] E. Cukierman, R. Pankov, K.M. Yamada, Cell interactions with three-dimensional matrices, *Curr. Opin. Cell Biol.* 14 (2002) 633–640, doi:[10.1016/S0955-0674\(02\)00364-2](https://doi.org/10.1016/S0955-0674(02)00364-2).
- [3] L.G. Griffith, M.A. Swartz, Capturing complex 3D tissue physiology *in vitro*, *Nat. Rev. Mol. Cell Biol.* 7 (2006) 211–224, doi:[10.1038/nrm1858](https://doi.org/10.1038/nrm1858).
- [4] C.M. Nelson, M.J. Bissell, Of extracellular matrix, scaffolds, and signaling: tissue architecture regulates development, homeostasis, and cancer, *Annu. Rev. Cell Dev. Biol.* 22 (2006) 287–309, doi:[10.1146/annurev.cellbio.22.010305.104315](https://doi.org/10.1146/annurev.cellbio.22.010305.104315).
- [5] J. Pape, M. Emberton, U. Cheema, 3D cancer models: the need for a complex stroma, compartmentalization and stiffness, *Front. Biotechnol.* 9 (2021) 1–8, doi:[10.3389/fbioe.2021.660502](https://doi.org/10.3389/fbioe.2021.660502).
- [6] B.N. Lourenço, G. Marchioli, W. Song, R.L. Reis, C.A. van Blitterswijk, M. Karpurien, A. van Apeldoorn, J.F. Mano, Wettability influences cell behavior on superhydrophobic surfaces with different topographies, *Biointerphases* 7 (2012) 1–11, doi:[10.1007/s13758-012-0046-6](https://doi.org/10.1007/s13758-012-0046-6).
- [7] S.J. Lee, J.S. Choi, K.S. Park, G. Khang, Y.M. Lee, H.B. Lee, Response of MG63 osteoblast-like cells onto polycarbonate membrane surfaces with different micropore sizes, *Biomaterials* 25 (2004) 4699–4707, doi:[10.1016/j.biomaterials.2003.11.034](https://doi.org/10.1016/j.biomaterials.2003.11.034).
- [8] F.M. Kievit, A. Cooper, S. Jana, M.C. Leung, K. Wang, D. Edmondson, D. Wood, J.S.H. Lee, R.G. Ellenbogen, M. Zhang, Aligned chitosan-polycaprolactone polyblend nanofibers promote the migration of glioblastoma cells, *Adv. Healthc. Mater.* 2 (2013) 1651–1659, doi:[10.1002/adhm.201300092](https://doi.org/10.1002/adhm.201300092).
- [9] D.O. Velez, B. Tsui, T. Goshia, C.L. Chute, A. Han, H. Carter, S.I. Fraley, 3D collagen architecture induces a conserved migratory and transcriptional response linked to vasculogenic mimicry, *Nat. Commun.* 8 (2017), doi:[10.1038/s41467-017-01556-7](https://doi.org/10.1038/s41467-017-01556-7).
- [10] S.K. Ranamukhaarachchi, R.N. Modi, A. Han, D.O. Velez, A. Kumar, A.J. Engler, S.I. Fraley, Macromolecular crowding tunes 3D collagen architecture and cell morphogenesis, *Biomater. Sci.* 7 (2019) 618–633, doi:[10.1039/c8bm01188e](https://doi.org/10.1039/c8bm01188e).
- [11] R.E. Burgesson, New collagens, new concepts, *Annu. Rev. Cell Biol.* 4 (1988) 551–577.
- [12] C. Frantz, K.M. Stewart, V.M. Weaver, The extracellular matrix at a glance, *J. Cell Sci.* 123 (2010) 4195–4200, doi:[10.1242/jcs.023820](https://doi.org/10.1242/jcs.023820).

- [13] E. Brauchle, J. Kasper, R. Daum, N. Schierbaum, C. Falch, A. Kirschniak, T.E. Schäffer, K. Schenke-Layland, Biomechanical and biomolecular characterization of extracellular matrix structures in human colon carcinomas, *Matrix Biol.* 68–69 (2018) 180–193, doi:10.1016/j.matbio.2018.03.016.
- [14] J. Yang, J. Richards, P. Bowman, R. Guzman, J. Enami, K. McCormick, S. Hamamoto, D. Pitelka, S. Nandi, Sustained growth and three-dimensional organization of primary mammary tumor epithelial cells embedded in collagen gels, *Proc. Natl. Acad. Sci. U. S. A.* 76 (1979) 3401–3405, doi:10.1073/pnas.76.7.3401.
- [15] D.F.D. Campos, A.B. Marquez, C. O'seanain, H. Fischer, A. Blaesser, M. Vogt, D. Corallo, S. Aveic, Exploring cancer cell behavior *in vitro* in three-dimensional multicellular bioprintable collagen-based hydrogels, *Cancers* 11 (2019), doi:10.3390/cancers11020180.
- [16] C.S. Szot, C.F. Buchanan, J.W. Freeman, M.N. Rylander, 3D *in vitro* bioengineered tumors based on collagen I hydrogels, *Biomaterials* 32 (2011) 7905–7912, doi:10.1016/j.biomaterials.2011.07.001.
- [17] X. Luo, E.L.S. Fong, C. Zhu, Q.X.X. Lin, M. Xiong, A. Li, T. Li, T. Benoukraf, H. Yu, S. Liu, Hydrogel-based colorectal cancer organoid co-culture models, *Acta Biomater* 132 (2021) 461–472, doi:10.1016/j.actbio.2020.12.037.
- [18] A. Nadu, L. Salomon, A. Hoznek, L.E. Olsson, F. Saint, A. De La Taille, A. Cicco, D. Chopin, C.C. Abbou, Changes in collagen metabolism in prostate cancer: a host response that may alter progression, *J. Urol.* 166 (2001) 1698–1701, doi:10.1016/s0022-5347(05)65656-x.
- [19] M.J. Paszek, N. Zahir, K.R. Johnson, J.N. Lakins, G.I. Rozenberg, A. Gefen, C.A. Reinhart-King, S.S. Margulies, M. Dembo, D. Boettiger, D.A. Hammer, V.M. Weaver, Tensional homeostasis and the malignant phenotype, *Cancer Cell* 8 (2005) 241–254, doi:10.1016/j.ccr.2005.08.010.
- [20] I. Avital, T.A. Summers, S.R. Steele, S. Waldman, A. Nissan, A.J. Bilchik, M. Protcic, Y.G. Man, B.L.D.M. Brücher, A. Stojadinovic, Colorectal cancer stem cells as biomarkers: where it all starts? *J. Surg. Oncol.* 107 (2013) 791–793, doi:10.1002/jso.23330.
- [21] A.G. Vaiopoulos, I.D. Kostakis, M. Koutsilieris, A.G. Papavassiliou, Concise review: colorectal cancer stem cells, *Stem Cells* 30 (2012) 363–371, doi:10.1002/stem.1031.
- [22] S.C. Kirkland, Type I collagen inhibits differentiation and promotes a stem cell-like phenotype in human colorectal carcinoma cells, *Br. J. Cancer.* 101 (2009) 320–326, doi:10.1038/sj.bjc.6605143.
- [23] C. Liu, H. Pei, F. Tan, Matrix stiffness and colorectal cancer, *Onco. Targets. Ther.* 13 (2020) 2747–2755, doi:10.2147/OTT.S231010.
- [24] F. Louis, S. Kitano, J.F. Mano, M. Matsusaki, 3D collagen microfibers stimulate the functionality of preadipocytes and maintain the phenotype of mature adipocytes for long term cultures, *Acta Biomater.* 84 (2019) 194–207, doi:10.1016/j.actbio.2018.11.048.
- [25] H. Liu, S. Kitano, S. Irie, R. Levato, M. Matsusaki, Collagen microfibers induce blood capillary orientation and open vascular lumen, *Adv. Biosyst.* (2020) <https://onlinelibrary.wiley.com/doi/abs/10.1002/adbi.202000038>.
- [26] Y. Naka, S. Kitano, S. Irie, M. Matsusaki, Wholly Vascularized Millimeter-Sized Engineered Tissues by Cell-Sized Microscaffolds, *Mater. Today Bio.* 6 (2020) 100054, doi:10.1016/j.mtbio.2020.100054.
- [27] N. Sasaki, H. Takeuchi, S. Kitano, S. Irie, A. Amano, M. Matsusaki, Dynamic analysis of Porphyromonas gingivalis invasion into blood capillaries during the infection process in host tissues using a vascularized three-dimensional human gingival model, *Biomater. Sci.* 9 (2021) 6574–6583, doi:10.1039/d1bm00831e.
- [28] E. Medico, M. Russo, G. Picco, C. Cancelliere, E. Valtorta, G. Corti, M. Buscarino, C. Isella, S. Lamba, B. Martinoglio, S. Veronese, S. Siena, A. Sartore-Bianchi, M. Beccuti, M. Mottolose, M. Linnebacher, F. Cordero, F. Di Nicolantonio, A. Bardelli, The molecular landscape of colorectal cancer cell lines unveils clinically actionable kinase targets, *Nat. Commun.* 6 (2015) 1–10, doi:10.1038/ncomms8002.
- [29] C.G. Hansen, Y.L.D. Ng, W.L.M. Lam, S.W. Plouffe, K.L. Guan, The Hippo pathway effectors YAP and TAZ promote cell growth by modulating amino acid signaling to mTORC1, *Cell Res.* 25 (2015) 1299–1313, doi:10.1038/cr.2015.140.
- [30] S.X. Ge, E.W. Son, R. Yao, iDEP: an integrated web application for differential expression and pathway analysis of RNA-Seq data, *BMC Bioinformatics* 19 (2018) 1–24, doi:10.1186/s12859-018-2486-6.
- [31] I. Minn, H. Wang, R.C. Mease, Y. Byun, X. Yang, J. Wang, S.D. Leach, M.G. Pomper, A red-shifted fluorescent substrate for aldehyde dehydrogenase, *Nat. Commun.* 5 (2014), doi:10.1038/ncomms4662.
- [32] S. Piccolo, T. Panciera, P. Contessotto, M. Cordenonsi, YAP/TAZ as master regulators in cancer: modulation, function and therapeutic approaches, *Nat. Cancer.* 4 (2023) 9–26, doi:10.1038/s43018-022-00473-z.
- [33] X. Sun, P.D. Kaufman, Ki-67: more than a proliferation marker, *Chromosoma* 127 (2018) 175–186, doi:10.1007/s00412-018-0659-8.
- [34] U. Gnther, M. Hofmann, W. Rudy, S. Reber, M. Zer, I. Hsusmann, S. Mstzku, A. Wenzel, A new variant of glycoprotein CD44 confers metastatic potential to rat carcinoma cells, 65 (1991) 13–24. [https://doi.org/10.1016/0092-8674\(91\)90403-L](https://doi.org/10.1016/0092-8674(91)90403-L).
- [35] O. Nagano, D. Murakami, D. Hartmann, B. De Strooper, P. Saftig, T. Iwatsubo, M. Nakajima, M. Shinohara, H. Saya, Cell-matrix interaction via CD44 is independently regulated by different metalloproteinases activated in response to extracellular Ca<sup>2+</sup> influx and PKC activation, *J. Cell Biol.* 165 (2004) 893–902, doi:10.1083/jcb.200310024.
- [36] O. Nagano, H. Saya, Mechanism and biological significance of CD44 cleavage, *Cancer Sci.* 95 (2004) 930–935, doi:10.1111/j.1349-7006.2004.tb03179.x.
- [37] Y. Yan, X. Zuo, D. Wei, Concise review: emerging role of CD44 in cancer stem cells: a promising biomarker and therapeutic target, *Stem Cells Transl. Med.* 4 (2015) 1033–1043, doi:10.5966/sctm.2015-0048.
- [38] K. Kobayashi, H. Matsumoto, H. Matsuyama, N. Fujii, R. Inoue, Y. Yamamoto, K. Nagao, Clinical significance of CD44 variant 9 expression as a prognostic indicator in bladder cancer, *Oncol. Rep.* 36 (2016) 2852–2860, doi:10.3892/or.2016.5061.
- [39] A. Yamaguchi, T. Urano, T. Goi, M. Saito, K. Takeuchi, K. Hirose, G. Nakagawara, H. Shiku, K. Furukawa, Expression of a CD44 variant containing exons 8 to 10 is a useful independent factor for the prediction of prognosis in colorectal cancer patients, *J. Clin. Oncol.* 14 (1996) 1122–1127, doi:10.1200/JCO.1996.14.4.1122.
- [40] Y. Kimura, T. Goi, T. Nakazawa, Y. Hirono, K. Katayama, T. Urano, A. Yamaguchi, CD44variant exon 9 plays an important role in colon cancer initiating cells, *Oncotarget* 4 (2013) 785–791, doi:10.18632/oncotarget.1048.
- [41] Y. Shen, X. Wang, J. Lu, M. Salfermoser, N.M. Wirsik, N. Schleussner, A. Imle, A. Freire Valls, P. Radhakrishnan, J. Liang, G. Wang, T. Muley, M. Schneider, C. Ruiz de Almodovar, A. Diz-Muñoz, T. Schmidt, Reduction of liver metastasis stiffness improves response to bevacizumab in metastatic colorectal cancer, *Cancer Cell* 37 (2020) 800–817.e7, doi:10.1016/j.ccell.2020.05.005.
- [42] L.A. Johnson, E.S. Rodansky, K.L. Sauder, J.C. Horowitz, J.D. Mih, D.J. Tschumperlin, P.D. Higgins, Matrix stiffness corresponding to strictured bowel induces a fibrogenic response in human colonic fibroblasts, *Inflamm. Bowel Dis.* 19 (2013) 891–903, doi:10.1097/MIB.0b013e3182813297.
- [43] F. Zanconato, M. Cordenonsi, S. Piccolo, YAP/TAZ at the roots of cancer, *Cancer Cell* 29 (2016) 783–803, doi:10.1016/j.ccell.2016.05.005.
- [44] M. Shibata, K. Ham, M.O. Hoque, A time for YAP1: tumorigenesis, immunosuppression and targeted therapy, *Int. J. Cancer.* 143 (2018) 2133–2144, doi:10.1002/ijc.31561.
- [45] H.J. Janse van Rensburg, X. Yang, The roles of the Hippo pathway in cancer metastasis, *Cell. Signal.* 28 (2016) 1761–1772, doi:10.1016/j.cellsig.2016.08.004.
- [46] J.S.A. Warren, Y. Xiao, J.M. Lamar, YAP/TAZ activation as a target for treating metastatic cancer, *Cancers* 10 (2018), doi:10.3390/cancers10040115.
- [47] S. Noguchi, A. Saito, T. Nagase, YAP/TAZ signaling as a molecular link between fibrosis and cancer, *Int. J. Mol. Sci.* 19 (2018), doi:10.3390/ijms19113674.
- [48] F. Zanconato, M. Forcato, G. Battilana, L. Azzolin, E. Quaranta, B. Bodega, A. Rosato, S. Bicciato, M. Cordenonsi, S. Piccolo, Genome-wide association between YAP/TAZ/TEAD and AP-1 at enhancers drives oncogenic growth, *Nat. Cell Biol.* 17 (2015) 1218–1227, doi:10.1038/ncb3216.
- [49] J. Rosenbluh, D. Nijhawan, A.G. Cox, X. Li, J.T. Neal, E.J. Schaffer, T.I. Zack, X. Wang, A. Tsherniak, A.C. Schinzel, D.D. Shao, S.E. Schumacher, B.A. Weir, F. Vazquez, G.S. Cowley, D.E. Root, J.P. Mesirov, R. Beroukhim, C.J. Kuo, W. Goessling, W.C. Hahn,  $\beta$ -Catenin-driven cancers require a YAP1 transcriptional complex for survival and tumorigenesis, *Cell* 151 (2012) 1457–1473, doi:10.1016/j.ccell.2012.11.026.
- [50] S. Dupont, Role of YAP/TAZ in cell-matrix adhesion-mediated signalling and mechanotransduction, *Exp. Cell Res.* 343 (2016) 42–53, doi:10.1016/j.yexcr.2015.10.034.
- [51] J. Cherfils, M. Zeghouf, Regulation of small GTPases by GEFs, GAPs, and GDIs, *Physiol. Rev.* 93 (2013) 269–309, doi:10.1152/physrev.00003.2012.
- [52] E.A. Clark, T.R. Golub, E.S. Lander, R.O. Hynes, Erratum: genomic analysis of metastasis reveals an essential role for RhoC (Nature (2000) 406 (532-535)), *Nature* 411 (2001) 974, doi:10.1038/35082119.
- [53] A. Malki, R.A. Elruz, I. Gupta, A. Allouch, S. Vranic, A.E. Al Moustafa, Molecular mechanisms of colon cancer progression and metastasis: recent insights and advancements, *Int. J. Mol. Sci.* 22 (2021) 1–24, doi:10.3390/ijms22010130.
- [54] N. Xie, C. Xiao, Q. Shu, B. Cheng, Z. Wang, R. Xue, Z. Wen, J. Wang, H. Shi, D. Fan, N. Liu, F. Xu, Cell response to mechanical microenvironment cues via Rho signaling: from mechanobiology to mechanomedicine, *Acta Biomater.* 159 (2023) 1–20, doi:10.1016/j.actbio.2023.01.039.
- [55] E. Jabbari, S.K. Sarvestani, L. Daneshian, S. Moeinzadeh, Optimum 3D matrix stiffness for maintenance of cancer stem cells is dependent on tissue origin of cancer cells, *PLoS ONE* 10 (2015) 1–21, doi:10.1371/journal.pone.0132377.
- [56] L.T. Senbanjo, M.A. Chellaiah, CD44: a multifunctional cell surface adhesion receptor is a regulator of progression and metastasis of cancer cells, *Front. Cell Dev. Biol.* 5 (2017), doi:10.3389/fcell.2017.00018.
- [57] N. Suwannakul, N. Ma, K. Midorikawa, S. Oikawa, H. Kobayashi, F. He, S. Kawanishi, M. Murata, CD44v9 induces stem cell-like phenotypes in human cholangiocarcinoma, *Front. Cell Dev. Biol.* 8 (2020) 1–15, doi:10.3389/fcell.2020.00417.
- [58] N. Sachs, H. Clevers, Organoid cultures for the analysis of cancer phenotypes, *Curr. Opin. Genet. Dev.* 24 (2014) 68–73, doi:10.1016/j.gde.2013.11.012.
- [59] G. Berx, A.M. Cleton-Jansen, F. Nollet, W.J.F. De Leeuw, M.J. Van De Vijver, C. Cornelisse, F. Van Roy, E-cadherin is a tumour/invasion suppressor gene mutated in human lobular breast cancers, *EMBO J* 14 (1995) 6107–6115, doi:10.1002/j.1460-2075.1995.tb00301.x.
- [60] T. Bogenrieder, M. Herlyn, Axis of evil: molecular mechanisms of cancer metastasis, *Oncogene* 22 (2003) 6524–6536, doi:10.1038/sj.onc.1206757.
- [61] V. Padmanaban, I. Krol, Y. Suhail, B.M. Szczepa, M. Aceto, J.S. Bader, A.J. Ewald, E-cadherin is required for metastasis in multiple models of breast cancer, *Nature* 573 (2019) 439–444, doi:10.1038/s41586-019-1526-3.
- [62] S. Tamura, T. Isobe, H. Ariyama, M. Nakano, Y. Kikushige, S. Takaishi, H. Kusaba, K. Takenaka, T. Ueki, M. Nakamura, K. Akashi, E. Baba, E-cadherin regulates proliferation of colorectal cancer stem cells through NANOG, *Oncol. Rep.* 40 (2018) 693–703, doi:10.3892/or.2018.6464.